Laser and Particle Beams (2001), *19*, 451–463. Printed in the USA.

Dynamics and stability of twisted-wire arrays

N.B. VOLKOV,[1] T.A. GOLUB,[2] R.B. SPIELMAN,[3] AND N.A. GONDARENKO[4]

[1]Institute of Electrophysics, Russian Academy of Sciences, Ural Division, Yekaterinburg, 620016, Russia
[2]GNG Enterprises Inc., P.O. Box 2068, Springfield, VA 22152, USA
[3]Sandia National Laboratories, Albuquerque, NM 87185-1194, USA
[4]Institute for Plasma Research, Maryland University, College Park, MD 20742, USA

(RECEIVED 22 May 2000; ACCEPTED 25 March 2001)

Abstract

A multiwire screw pinch, a variant of a *z*-pinch load, is proposed as a means for further improvement of load performance for high-current 100-ns pulsed-power generators used for terawatt X-ray radiation. Wires twisted along a curved load surface are suggested to be an effective way to create an axial magnetic field and to generate and to maintain rotation of the subsequently formed plasma shell due to conservation of angular momentum. A multiwire screw pinch is predicted to mitigate the growth of the magneto-Rayleigh–Taylor instabilities, to provide a higher pinch compression ratio and more effective X-ray generation compared to classical *z*-pinch loads. A model based on the self-consistent simulation of the dynamics of a twisted plasma shell and the development of Rayleigh–Taylor (R-T) perturbations on a plasma surface is proposed to quantitatively study the effect of various physical factors on the generation of X rays. The model provides us with a tool for the analysis of processes that occur during the implosion of the plasma-shell–wire-core system. We plan for the R-T perturbations to break through the plasma shell at the moment when the internal radius of a shell becomes zero, where the greatest possible values of kinetic energy and X-ray radiation power ought to be obtained. The results of numerical simulations for the Sandia National Laboratories' Z generator are presented and discussed.

1. INTRODUCTION

Experiments and simulations (Davis *et al.*, 1997; Deeney *et al.*, 1998; Spielman *et al.*, 1998) have shown that *z* pinches, formed by multiwire arrays and nested multiwire arrays, are effective sources of terawatt levels of X-ray radiation. For small numbers of wires, the plasma coronas of individual wires are not overlapped for most of the implosion, and the instabilities developed in each wire do not exhibit mutual influence. The case of a wire array having a large number of wires is of particular interest, as Sandia National Laboratories' (SNL) experiments (Spielman *et al.*, 1998) demonstrated a significant improvement in the uniformity of plasma parameters over the load length and optimized the generation of X-ray radiation when the number of wires $N = 200$–300. In this case, the plasma coronas of separate wires are overlapped and merge into a shell (Gus'kov *et al.*, 1998; Shelkovenko *et al.*, 1998; Spielman *et al.*, 1998; Pikuz *et al.*, 1999) which then implodes. The total current of the load flows through the shell. The amount of evaporated material depends on the electrical conductivity and the equation of state of the wire material (Gus'kov *et al.*, 1998; Shelkovenko *et al.*, 1998; Pikuz *et al.*, 1999). In Cornell University's experiments (Shelkovenko *et al.*, 1998; Pikuz *et al.*, 1999) with exploding tungsten wires, about 20% of the initial wire mass forms a plasma shell while the diameter of the dense wire core is 4–10 times the initial diameter of the wire. In SNL experiments (Spielman *et al.*, 1998) the magnitude of current flowing through each tungsten wire in the array is comparable with that in Cornell University's experiments where the wire diameter varies from 7.5 μm to 15 μm, the initial wire-array diameter is 4 cm, and the final diameter of a wire-array pinch plasma is 1.6 mm. Simple calculations for a lower estimate of the core diameter show that the cores of $N = 240$ wires, 7.5 μm in diameter, are overlapped only at the stagnation stage.

Marder and Desjarlais (1998) provided a physical explanation for the improvement in X-ray radiation as the number of wires increases to greater than 100. In that case, the kink instability in each wire goes away and the instability in the array reduces to the classical R-T and in this limit, the *z*-pinch plasma appears more stable. But the problem still remains: R-T instabilities develop as the plasma shell is formed and implodes and limit the X-ray radiation power. This problem becomes more severe for the long-pulse *z*-pinch implosions

Address correspondence and reprint requests to: N.B. Volkov, Institute of Electrophysics, Russian Academy of Sciences, Ural Division, Amundsen Sreet, 106, Yekaterinburg, 620016, Russia. E-mail: nbv@ami.uran.ru

(>150 ns) that are being investigated at the present time (Deeney *et al.*, 1999).

While it has been shown experimentally (Spielman *et al.*, 1998) that an increase in wire number improves uniformity along the load axis, time-resolved X-ray images of a *z* pinch at the stagnation stage in the X-ray range 1–3 keV demonstrate existence of bright spatially ordered structures along the pinch axis (Spielman *et al.*, 1998), which clearly show the pinch nonuniformities. Experiments (Branitskii *et al.*, 1999) aimed at studying of the cold-start effects on plasma liner implosions at "Angara 5-1" revealed a similar picture. Branitskii *et al.* (1999) demonstrated that cold-start effects promote the development of instabilities and magnetohydrodynamic (MHD) turbulence in a *z*-pinch plasma and they suggest that record values of X-ray radiation achieved in experiments (Spielman *et al.*, 1998) are likely caused by these instabilities and strong turbulent mixing. The plasma in these "bright" spots has the highest temperature, so the plasma temperature distribution follows the same structural pattern. Earlier studies of laminar-turbulent transition in plasma-like media (Volkov & Zubarev, 1995; Iskoldsky *et al.*, 1996) showed that creation of ordered spatial structures is caused by the formation and the development of nonlinear dynamics of large-scale vortices. Therefore, one can speculate that the experiments (Spielman *et al.*, 1998) demonstrate the existence of developed, macroscopic turbulence in multiwire *z*-pinch plasmas at stagnation. Using a phenomenological approach, Thornhill *et al.* (1994) showed that turbulence is an important factor for achieving higher X-ray radiation power of plasma in the kiloelectron volt region. A similar idea was proposed by Rudakov and Sudan (1997), where a simplified model of MHD turbulence in radiating *z* pinches was presented. We suggest that pinch designs that promote large-scale space turbulence, resulting in strong turbulent flow and more effective conversion of kinetic energy into thermal energy and an increase in X-ray radiation, would be one way to further improve *z*-pinch load performance (Volkov *et al.*, 1999*a*). The main obstacle here is the Raleigh–Taylor instabilities that could destroy both metallic and plasma liners during the implosion. However, if the beginning of the plasma shell destruction is synchronized in time to the beginning of the stagnation, then the R-T instabilities could increase the efficiency of conversion of the liner kinetic energy into the thermal energy and the X-ray radiation energy by a manifestation of turbulence in the plasma at the stagnation stage.

It is well known (Chandrasekhar, 1961) that an axial magnetic field, plasma rotation, and velocity shear each reduce the growth rate of the classical R-T instability. This is the reason why various techniques to generate an axial magnetic field and rotation of plasmas generated by multiwire loads are being seriously considered. The nonzero curvature of a load along with an axial magnetic field promotes an increase in the rotation velocity (Golub *et al.*, 1997*a*). In addition, it has been shown (Golub *et al.*, 1997*a*) that an axially curved surface of a *z*-pinch load decreases the growth rate of the R-T instability through velocity shear. A solenoidal return current cage was suggested as one source of an axial field (Sorokin & Chaikovsky, 1993; Golub *et al.*, 1997*a*). Obviously, the effect of this source of axial magnetic field decreases rapidly as the liner moves away from the return current cage during implosion. Therefore, it is desirable to find more efficient alternatives for creating an axial magnetic field. One of the possible ways is to use a specially designed load with wires placed under some angle to the generatrix of a cylindrical surface with either zero or a finite curvature. We refer to such a configuration as a multiwire screw pinch (S pinch; Volkov *et al.*, 1999*b*). One advantage of the S pinch is the fact that the wires creating the axial magnetic field collapse to the load axis with high radial velocity and, due to the curvature of the load surface along which wires are placed, an azimuthal component of the Lorentz force appears and load rotation occurs. The eventual formation of a plasma shell removes the azimuthal force promoting rotation. However, the plasma rotation does not stop instantly. Moreover in low dissipation media with low viscosity, the angular velocity increases with the decrease of load radius due to the conservation of angular momentum. The increasing angular velocity results in a decrease of the R-T growth rate of large wavelength instabilities (Thornhill *et al.*, 1994) and it increases the rate of plasma turbulent flow. Therefore, conversion of kinetic energy into thermal radiation energy at the stagnation stage is predicted to become more efficient. It is impossible to obtain such favorable conditions with classical *z*-pinch loads.

The idea of using an axial magnetic field for stabilization of the R-T instabilities was implemented earlier in various experiments (Wessel *et al.*, 1986*a*, 1986*b*; Sorokin *et al.*, 1991; Oreshkin, 1995; Gasque *et al.*, 1998). Various effects of the injected B_z in a gas-puff *z* pinch are described in detail (Wessel *et al.*, 1986*a*, 1986*b*; Sorokin *et al.*, 1991), including the increase in the final emitting radius of the pinch, the decrease in the X-ray intensity at pinching and stabilization of the plasma column. Stabilization was noticeable by injecting even a small amount of axial field, $B_0 = 1$ kG.

The stabilizing effect of the axial magnetic field on gas-puff *z* pinch was also reported by Gasque *et al.* (1998). However, measured soft X-ray yield in the range of $190 < h\nu < 288$ eV in experiment (Wessel *et al.*, 1986*a*) was only half of that for the implosion without axial magnetic field due to the fact that the energy of the compressed axial magnetic field constituted a significant portion of the load energy.

In experiments with a helium plasma liner (Oreshkin, 1995) a stable implosion was observed in the presence of a relatively weak axial magnetic field (0.15–0.3 T).

A solenoidal-current return can was used in experiments (Sorokin & Chaikovsky, 1993) along with constantly applied axial magnetic field for stabilization of krypton-filled *z*-pinch load. It was shown that a smaller value of B_z is sufficient for the stabilization of large-scale R-T instabilities in the initial stage of compression when B_z is applied along with solenoidal current return can. The combination of two stabilization technique enables Sorokin and Chai-

https://doi.org/10.1017/S0263034601193134 Published online by Cambridge University Press

kovsky (1993) to achieve the higher final compression ratio of the *z*-pinch plasma (~50). No increase in X-ray power was demonstrated in this configuration. The puff-on-puff configuration was applied in order to increase the efficiency of energy coupling between the pulse-power generator and the inner liner. The 1-D RMHD calculations (Gersten *et al.*, 1986) for the conditions of experiments (Sorokin & Chaikovsky, 1993) with the axial magnetic field revealed that the energy of the compressed axial magnetic field makes up to 80% of the total energy delivered to the gas-puff load, while over 50% delivered to the puff-on-puff load is converted into thermal energy. The series of intense shock waves pass through the inner liner while only one weak shock wave passes through the outer liner, and the conversion of the kinetic energy into the thermal energy is more effective in the puff-on-puff load. Therefore, the X-ray losses in the puff-on-puff load are a factor of two higher than those losses for the single-puff load. Gersten *et al.* (1986) suggested that the axial magnetic field dissipates in the volume between two layers, and this results in the increase of X-ray yield.

Liberman *et al.* (1999) suggested the use of twisted back current rods to create the hybrid z–θ pinch on the Blackjack 3 pulsed-power generator to achieve high stability and high compression ratio. It should be noted, it is really a controversial task to create the necessary axial magnetic field with twisted return current rods to provide stable pinch and at the same time to achieve efficient energy coupling between the pulse generator and the load. In addition, Volkov (1999) noted that, contrary to the gas-puff or plasma *z* pinches, the presence of an external magnetic field has a destabilizing effect on the implosion of a wire array. This conclusion was based on the analysis on wire array implosions with a relatively small number of wires, up to 48. The number of wires in the experiments (Liberman *et al.*, 1999) was in this range.

In the case of S-pinch load design, a special wire configuration will generate an initial B_z, which, in combination with the load curvature, will create and maintain the rotation of the formed plasma shell. In addition to the initial twist of the multiwire load, we propose to use the current return can with several slots placed at an angle to the axis of the can. This would create a constantly acting azimuthal Lorentz force, promoting the initial rotation of a multiwire *z*-/S-pinch load. Though the magnitude of this force on the load will decrease as the load moves away from the return current can during implosion, this force will be present during the entire time of the implosion and it will contribute to the creation of an angular momentum of the load even after the plasma shell is formed. This Lorentz force will partially mitigate the growth rate of the R-T instabilities and localize them in the central cross section of the load. We also suggest that strong turbulent mixing will result in an increase in the rate of magnetic field dissipation and, therefore, in an increase of the X-ray yield (Volkov, 1999; Volkov *et al.*, 1999*a*).

The process of a twisted multiwire pinch implosion can be subdivided into three stages: the stage of wire implosion and rotation that occurs up to the moment of plasma shell formation; the stage of compression of the current shell pushing ahead of the wire cores and rotation of the shell with wire cores, maintained by the radial compression; and the stagnation stage of plasma with developed macroscopic turbulence when kinetic energy is converted into radiation energy.

Multidimensional radiation hydrodynamic Reynolds-type equations could adequately describe the latter stagnation stage (Volkov, 1999). In this review, we consider zero-dimensional (0-D) models to study the dynamics of a twisted *z*-pinch load during the first stage prior to stagnation. A zero-dimensional model for the dynamics of a twisted plasma shell and the Rayleigh-Taylor perturbations on a plasma surface are developed for the simulation of the second stage. The model is applied to study the effect of initial wire twist on the dynamics of the large wavelength R-T instability growth and X-ray radiation.

2. MODELS FOR THE SIMULATION OF TWISTED-WIRE-ARRAY DYNAMICS

2.1. A zero-dimensional model of the first stage of twisted-wire-array dynamics

Classical mechanics (Landau & Lifschits, 1973) is a suitable approximation for the description of a wire implosion onto the load axis before the formation of a plasma shell because the plasma coronas of separate wires have not yet merged into a plasma shell and the wire diameters are small [in experiments (Spielman *et al.*, 1998), it is about 1–10 μm]. The 0-D equations of motion describing the implosion of a wire system can be written as

$$\begin{cases} \dfrac{d^2R}{dt^2} = \dfrac{I^2}{2m}\dfrac{\partial L_{eff}}{\partial R}, & (1) \\ \dfrac{d^2\beta}{dt^2} = -\dfrac{\Omega_m V}{R} + \dfrac{I^2}{mR}\dfrac{\partial L_{eff}}{\partial \beta}. & (2) \end{cases}$$

where V, R, Ω_m, β, m, I, and L_{eff} are the radial velocity, the instantaneous radius of the load, the angular velocity of rotation, the twisting angle, the total line mass of wires, the total current, and the effective inductance of a load, respectively. All variables are in SI units. The dependence of the angular velocity and the radius on the z coordinate can be approximated by the expressions $\Omega(z,t) = \Omega_m(t)\sin(\pi z/l)$ and $R(z,t) = R(t) - \Delta\cdot\cos(\pi z/l)$, respectively. In the latter formula, Δ is the parameter describing the curvature of the load surface and l is the length of a load.

The circuit equation can be combined with the equations of motion giving

$$d(I(L_{eff} + L_0))/dt + R_0 I = U(t), \quad (3)$$

where $U(t)$ is the given input voltage waveform, and R_0, L_0 are the resistance and the inductance of the external circuit.

https://doi.org/10.1017/S0263034601193134 Published online by Cambridge University Press

For the scaling of an S-pinch load during the first stage of the implosion, we use Eqs. (1)–(3). As in the experiments (Spielman *et al.*, 1998), a higher rate of increase of the kinetic energy corresponds to a higher X-ray radiation output. Therefore, we define a criterion for optimization as dW_k/dt, where W_k is the kinetic energy of a load. Since the first stage of compression is relatively short in duration, we can estimate the load inductance with $L_{eff} = \cos\beta L_\varphi + \sin\beta L_z$, where L_φ is the effective inductance of multiwire S pinch,

$$L_z = \frac{2\pi\mu_0 R_T}{l^2}\int_{-l/2}^{l/2} \frac{(R_T - R(x))dz}{1 + 2.5\,\dfrac{R_T - R(z)}{R_T} + \dfrac{2(R_T - R(z))}{l}\left(\ln\dfrac{\pi R_T}{R_T - R(z)} - 0.47 - q\left(\dfrac{l}{R_T}\right)\right)} \tag{4}$$

is the inductance of a one-loop solenoid with a very thin wall in the conducting screen (Schneerson, 1992), and $q(l/R_T) = 2.276\exp(-1.764l/R_T)$ is the approximation of numerical results.

We substitute the coaxial system of N wires and coaxial return current can with a system of $N * N$ contours from parallel wires, the same current, I/N^2, passes through each contour. Due to the axial symmetry of the system, the magnetic flux in each contour is

$$\Phi = I/N^2 \sum_{j=1}^{N}\sum_{j'=1}^{N} L_{ii';jj'} = L_\varphi I.$$

For a system of straight wires or a flat surface we use (Neyman & Demirchan, 1981; Golub *et al.*, 1999*a*)

$$L_{ii';jj'} = \frac{\mu_o l}{2\pi}\ln\frac{r_{ij'}r_{i'j}}{r_{ij}r_{i'j'}},$$

then

$$L_{eff} = \frac{\mu_0 l}{2\pi N^2}\sum_{j=1}^{N}\sum_{j'=1}^{N}\ln\frac{r_{ij'}r_{i'j}}{r_{ij}r_{i'j'}},$$

where r_{ij} denotes the distance between the ith and jth wires, indexes i and j without a prime relate to load wires, and indexes with a prime relate to virtual wires of the return current cage. For a curved surface, the expression for effective inductance of a multiwire S pinch is

$$L_\varphi = \frac{\mu_0}{2N^2\pi}\int_{-l/2}^{l/2}\sum_{j=1}^{N}\sum_{j'=1}^{N}\ln\frac{r_{ij'}(z)r_{i'j}(z)}{r_{ij}(z)r_{i'j'}}\,dz.$$

In our first consideration of the second stage of an S-pinch dynamics, we neglect here, for simplicity, the influence of shell thickness on the growth rate of the R-T instability, though we emphasize that its effect on R-T instability development is significant at this stage and should be studied in the future for a quantitative description of an S-pinch load prior to the stagnation stage. We use Eqs. (1)–(4) for the approximate description of the implosion of a plasma shell with wire cores, but the second term in the right-hand side of Eq. (2) should be omitted. Then the angular velocity of rotation increases as a shell implodes. After the plasma shell is formed, we use the following formula for the effective inductance of a load:

$$L_{eff} = L_\varphi = \frac{\mu_0}{2\pi}\int_{-l/2}^{l/2}\ln(R_T/R(z,t))\,dz,$$

where R_T is the radius of the return current can.

2.2. A model of the plasma-wire-core implosion and the R-T instabilities

Let us consider the average radial motion of a plasma shell with wire cores prior to stagnation. We assume axial and azimuthal symmetry of the load, inertia of the wire cores, plasma incompressibility, and zero magnetic field inside of a shell due to the skin effect. The equation of motion for the plasma shell is (Volkov *et al.*, 1976)

$$\frac{\partial V}{\partial t} + \frac{\partial}{\partial r}\left(\frac{V^2}{2} + \frac{r^2\Omega_m^2}{2}\right) = -\frac{\partial}{\partial r}\left(\frac{P}{\rho}\right) - \frac{B}{\mu_0\rho}\left(\frac{\partial B}{\partial r} + \frac{B}{r}\right), \tag{5}$$

where V, r, Ω_m, P, ρ, B, and μ_0 are the velocity of the shell, the radius of the shell, the twist angle, the pressure, the plasma shell density, the magnetic field, and the free space permeability, respectively.

The above assumptions can be written as

$$V_i R_i = V_e R_e = Vr \tag{6}$$

$$s_0 = \pi(R_{e0}^2 - R_{i0}^2) = \pi(R_e^2 - R_i^2) = const, \tag{7}$$

where V_i, R_i, V_e, R_e, and s_0 are the internal radial velocity, the internal radius of the shell, the external radial velocity, the external radius of the shell, and the area of the shell cross section, respectively.

To obtain the ordinary differential equation for an average internal velocity, we use the assumption that the magnetic field inside the shell is equal to zero, and also we take into account the inertia of the wire cores. Integrating Eq. (1) over the radius, taking into account Eqs. (2) and (3), we obtain

https://doi.org/10.1017/S0263034601193134 Published online by Cambridge University Press

$$\frac{dV_i}{dt} = \frac{V_i^2\left(\frac{s_0}{\pi R_i^2}\right) - \ln(\xi) - \frac{\Omega_m^2 s_0}{\pi} - \frac{\mu_0 I^2}{2\pi^2 \rho R_i^2 \xi}}{R_i\left(\ln(\xi) + (\sqrt{\xi} - 1)\frac{\rho}{\rho_c}\right)} \tag{8}$$

$$R_e = R_i\xi, \qquad V_e = \frac{V_i}{\xi}, \qquad \xi = \sqrt{1 + \frac{s_0}{\pi R_i^2}} \tag{9}$$

$$\frac{d^2\beta}{dt^2} = -\frac{\Omega_m V_i}{R_i}, \tag{10}$$

where I, ρ_c, and β are the current through the load, the wire core density, and the twist angle, respectively.

Let us represent the coordinate of a point on the load surface as the sum of coordinates of a point on the unperturbed surface $\Re_m(z,t)$ and the amplitude of a short wavelength perturbation $\eta(z,t)$:

$$\Re(z,t) = \Re_m(z,t) + \eta(z,t). \tag{11}$$

When the wire length is fixed, the twisting of an originally cylindrical wire array results in the curvature of the load surface. This surface curvature promotes the localization of the R-T instabilities in the central cross section of the load. This fact is supported by 2-D MHD calculations presented by Douglas *et al.* (1997). Therefore, we can take into account the surface curvature effect by representing the perturbation as follows:

$$\eta(z,t) = F\left(\frac{\partial \Re_m}{\partial z}\right)\eta_{fl}(z,t) + o(\epsilon), \tag{12}$$

where the localization function

$$F\left(\frac{\partial \Re_m}{\partial z}\right) = \exp(-\beta^2\bar{\delta}^2\alpha^2\sin(\alpha z)),$$

$$\bar{\delta} = k\delta, \qquad \alpha = k_0\lambda,$$

is the wavepacket envelope function for the short wavelength perturbations, so that perturbations approach zero near the electrodes for a curved surface, and $\eta_{fl}(z,t)$ is the perturbation on the flat surface. The last term in the right-hand side of Eq. (12) takes into account the coupling of modes with $k_0 = \pi/l$ and short wavelength perturbations. We neglect this term in our further analysis.

Using a piece-wise approximation as was done by Fermi (1972), we represent the perturbation component for the flat surface as

$$\eta_{fl}(\bar{z},t) = X_{sp}(t)\sum_{i=1}^{n+1}(H(\bar{z} - \bar{z}_{2i-1}) - H(\bar{z} - \bar{z}_{2i})) - X_b(t)\sum_{i=1}^{n+1}(H(\bar{z} - \bar{z}_{2i}) - H(\bar{z} - \bar{z}_{2i+1})), \tag{13}$$

where $H(\bar{z} - \bar{z}_i)$ is the Heaviside function, and the points $\bar{z}_i$, $i = 1,2,\ldots,2n+2$ are the beginning and end points of the spike or the bubble of the instability. The dimensionless amplitude of the spike and the bubble of the R-T instability are $\eta_{fl} = k\eta$, $\bar{z} = z\lambda^{-1}$. Introducing a dimensionless height and width of the spike $X_{sp} = k\eta_{sp}$, $X_b = k\eta_b$, we write the equations for dynamics of the spike and the bubble. These equations are similar to Baker and Freeman's nonlinear model for the R-T instabilities in ICF targets (Baker & Freeman, 1980) that was later adopted by Loskutov and Luchinsky (1995) for analysis of the R-T instabilities in imploding liners. It is assumed (Loskutov & Luchinsky, 1995) that the bubble and the spike of the R-T instabilities grow independently. This assumption is not valid for incompressible fluid, so we use the bubble-spike growth equations as follows:

$$\frac{dV_1}{dt} = -\frac{f(X_{sp} - X_0)}{(1 + X_{sp})^2}V_1^2 - \frac{2V_1V_i}{R_i\xi} + \frac{kf(X_{sp})}{\xi}\left(g_i + \frac{V_i^2 s_0}{\pi R_i^3 \xi}\right), \tag{14}$$

where V_1 is the growth rate of the spike amplitude,

$$\frac{dX_{sp}}{dt} = V_1, \tag{15}$$

where $f(x) = 1 - \exp(-x)$ and $g_i = dV_i/dt$,

$$\frac{dV_2}{dt} = -\frac{(h_bV_1 + X_{sp}V_2)^2}{X_{sp}h_b^2}f\left(\frac{X_{sp}}{h_b}\right) - \frac{2V_2V_i}{R_i\xi} + \frac{kh_b}{X_{sp}\xi}\left(g_i + \frac{V_i^2 s_0}{\pi R_i^3\xi}\right)\left(h_b f\left(\frac{X_{sp}}{h_b}\right) - f(X_{sp})\right) + \frac{h_bV_1^2}{X_{sp}}\frac{f(X_{sp} - X_0)}{(1 + X_{sp})^2} - \frac{2V_2(h_bV_1 + X_{sp}V_2)}{X_{sp}h_b}, \tag{16}$$

where V_2 is the growth rate of the spike width,

$$\frac{dh_{sp}}{dt} = V_2. \tag{17}$$

The amplitude, X_b, and the width, h_b, of a bubble are

$$X_b = \frac{X_{sp}h_{sp}}{1 - h_{sp}}, \quad h_b = 1 - h_{sp}. \tag{18}$$

The initial values for Eqs. (14)–(18) are given by

$$h_0 = h_{sp}(t = t_0) = \tfrac{1}{2}, \qquad X_{sp}(t = t_0) = X_0.$$

https://doi.org/10.1017/S0263034601193134 Published online by Cambridge University Press

2.3. A model of the implosion of a twisted wire array pinch with the current return can having inclined slots

We limit our consideration with the 0-D model of the load dynamics which was described in the previous subsection. We present in this section the inductance expressions modified for the load with current return can with the inclined slots (Golub *et al.*, 1999*b*).

We substitute the coaxial system of N wires and coaxial return current can with a system of $N * N_{sl}$ contours from N wires of the array and N_{sl} filaments which represent the stripes of can material between slots. The same current, $I/(N * N_{sl})$, passes through each contour. Using the axial symmetry of the system and an expression for inductance of each contour (Golub *et al.*, 1999*a*) we can write inductance for a system of straight wires or a flat surface as

$$L_{eff} = \frac{\mu_0 l}{2\pi} \frac{1}{NN_{sl}} \sum_{j=1}^{N} \sum_{j'=1}^{N_{sl}} \ln \frac{r_{ij'} r_{i'j}}{r_{ij} r_{i'j'}}, \tag{19}$$

where r_{ij} denotes the distance between the ith and jth wires, indexes i and j without a prime relate to load wires, and indexes with a prime relate to filaments of the return current can.

For a curved surface, the expression for the effective inductance of a multiwire S pinch becomes

$$L_{\varphi} = \frac{\mu_0}{2NN_{sl}\pi} \int_{-l/2}^{l/2} \sum_{j=1}^{N} \sum_{j'=1}^{N_{sl}} \ln \frac{r_{ij'}(z) r_{i'j}(z)}{r_{ij}(z) r_{i'j'}(z)} dz.$$

We use Eqs. (1)–(4) for the approximate description of the implosion of a plasma shell with wire cores, but the second term in the right-hand side of Eq. (2) should be omitted. Then the angular velocity of rotation increases as a shell implodes.

After the plasma shell is formed, we use the following formula for the effective inductance of a load: $L_{eff} = L_{p1} + \sin(\alpha)(L_{p2} + L_{p3})$, where R_T is the radius of the return current cage, α is the slot inclination angle, L_{p1} is the inductance related to azimuthal field of the return current solenoid and a plasma shell of arbitrary surface $R(z,t)$ (Golub *et al.*, 1997*a*):

$$L_{p1} = \frac{\mu_0}{2\pi} \int_{-l/2}^{l/2} \ln(R_T/R(z,t)) dz;$$

L_{p2} is the inductance related to axial magnetic field (Golub *et al.*, 1997*a*):

$$L_{p2} = \frac{r\pi^2}{\int_{-l/2}^{l/2} \frac{dz}{R_T^2 - R(z,t)^2}};$$

and L_{p3} is the inductance related to the radial magnetic field:

$$L_{p3} = 2\pi^2 \frac{\int_{-l/2}^{l/2} \frac{R(z,t)^2 (R_T^2 + R(z,t)^2) \left(\frac{\partial R(z,t)}{\partial z} \right)^2 dz}{(R_T^2 - R(z,t)^2)^3}}{\left(\int_{-l/2}^{l/2} \frac{dz}{R_T^2 - R(z,t)^2} \right)^2},$$

where R_s is the solenoid radius or return current radius R_T and $R(z,t)$ is the radius of the pinch load depending on the z coordinate. The factor $\sin(\alpha)$ is introduced to take into account the difference of the return current can with inclined slots from the return current solenoid.

A model based on a self-consistent simulation of the dynamics of a twisted plasma shell and the development of the Rayleigh-Taylor perturbations on a plasma surface is described in detail in Section 2.1 and was used in our simulations to scale the shell dynamics in the presence of the current return can with the inclined slots.

3. NUMERICAL SIMULATION

The dynamics of various configurations of S-pinch loads with curved surfaces and twisted wires was simulated numerically and compared with the performance of a classical z pinch. In all calculations, we used the Z circuit (Spielman *et al.*, 1998) with $L_0 = 11.28$ nH, $R_0 = 0.12$ Ω, given input voltage waveform, 4-mg mass of the load 2 cm long, 3 cm in diameter. We estimated 122 ns as the moment in time when the coronas of 100 separate tungsten wires overlap and merge into a plasma shell, using a 1-D MHD code for simulation of the "cold start" problem (Golub *et al.*, 1997*b*). The parameter Δ denotes the initial difference between the maximum load radius on the electrodes and the minimum load radius in the central cross section (Fig. 1). The initial load radius on the electrode was fixed at 1.5 cm in all calculations, and we controlled the initial load curvature by varying the parameter Δ. Thus, $\Delta = 0.0$ corresponds to a flat surface, $\Delta = 0.1$ cm means that load radius in the central cross section is 1.4 cm, that is, the surface is curved just a little bit, and $\Delta = 0.7$ cm relates to a highly curved surface when the radius of the central cross section of the load is almost a half value of the load radius on the electrodes. The parameter β describes the load twist angle (Fig. 1). The initial value β_0 determines the angle of the initial placement of the wires along the load surface. Thus, for $\beta_0 = 0.0$, we have wires stacked straight which in combination with $\Delta = 0.0$ relates to a classical z pinch. The case $\beta_0 = 0.05$ relates to the configuration of the load with wires initially placed in a 4.3° angle to the cylindrical surface generatrix. The derivative of the parameter β is an angular velocity.

Numerical simulations with 0-D implosion dynamics model were performed for a classical z-pinch load and for an S-pinch load with initial twist ranging from 0.02 to 0.15 and initial curvature ranging from 0.05 cm to 0.7 cm. Figure 2

https://doi.org/10.1017/S0263034601193134 Published online by Cambridge University Press

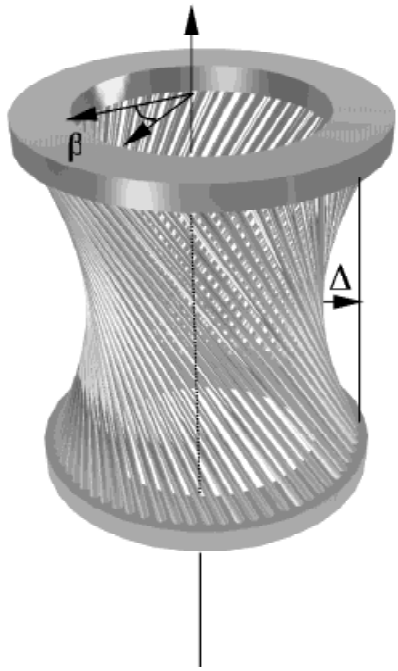

Fig. 1. Schematic design of an S-pinch load. Parameter of twisting, β, is an angle of rotation of the load relative to the fixed central cross section of the load. Parameter of load curvature, Δ, is defined by the displacement of outer load surface from flat surface.

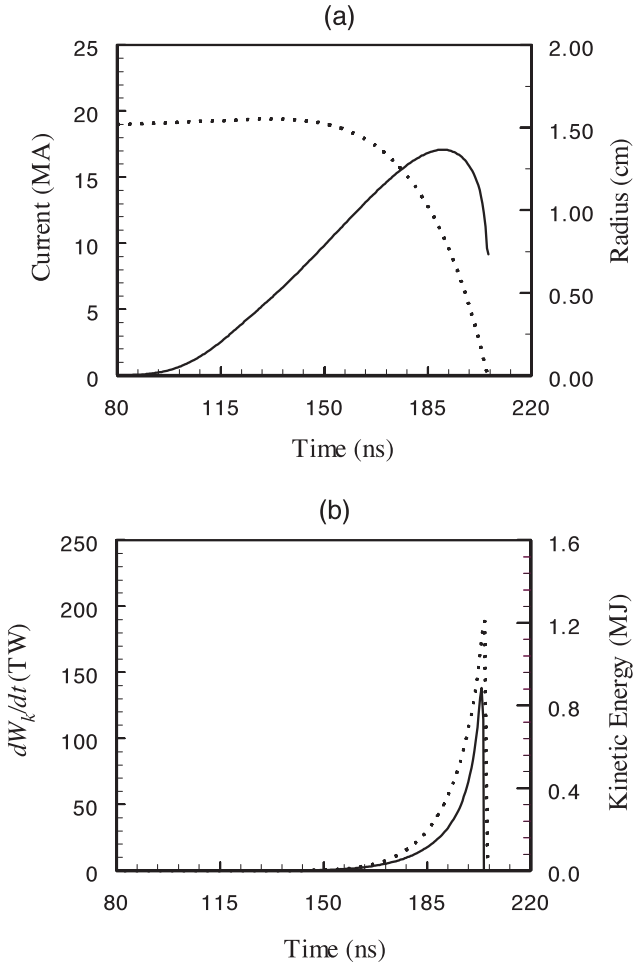

Fig. 2. Dynamics of a classical *z*-pinch load: (a) the time histories of the load current (solid line) and maximum load radius (dotted line); (b) time histories of the radial kinetic energy W_k (dotted line) and the mechanical power W_k/dt (solid line).

shows the dynamics of a classical *z* pinch and Figure 3 demonstrates the performance of an S pinch for $\Delta = 0.2$ and $\beta_0 = 0.05$.

The results of numerical 0-D simulations prove the concept that an S-pinch design could provide a dramatic effect on load performance. The higher rate of rise of load inductance for an S pinch determines the more effective conversion of electrical energy of the driver into the kinetic energy of the load. Both the peak kinetic energy W_k and the rate of rise of the kinetic energy dW_k/dt increase significantly compared to classical *z*-pinch load (Figs. 2 and 3). Quantitative estimations do not reflect the real scenario in energy conversion as our simulations did not account for radiative losses.

Simulations revealed that the effect of parameter Δ dominates the influence of the initial twist angle. Therefore, the initial curvature of the load is suggested as the principal control parameter. If we choose the highest peak and the rate of rise of the kinetic energy, as an optimum criterion, then we find $\Delta = 0.2$ and $\beta_0 = 0.05$ as the optimum.

Equations (8)–(18) were used for self-consistent simulations of the dynamics of the plasma shell and the development of the R-T instabilities on a plasma surface. Various configurations of twisted loads were simulated numerically and compared with the performance of a classical *z* pinch with straight cylindrical wires. The initial shell thickness was set at 0.9 mm, and the initial amplitude of spike and bubble at 0.02 mm. The 2-D MHD calculations for uniform-fill loads (Douglas *et al.*, 1997) show that the curved load surface promotes the mitigation of the short-wavelength R-T instabilities, the large wavelength instabilities dominate, and the larger the surface curvature, the smaller the range of wavelengths for the R-T instabilities developed during implosion. Thus, we used wave numbers $k = 2\pi n/l$, $n = 5, 7, 9, 11$ in our simulations. Constant values of 0.01 g/cm^3 for plasma density and 1 g/cm^3 for wire core density were used in the calculations. These values are comparable with estimates based on experimental measurements (Shelkovenko *et al.*, 1998; Pikuz *et al.*, 1999), where the value of current flowing through the 7.5-μm diameter tungsten wire is the same as that in the Z experiments.

Time histories of the current through the load and the wire array radius near the electrodes along with the amplitudes of a spike and a bubble are shown in Figure 4. The calculations showed that linear theory gives too high an estimate for the growth rate of the R-T instability amplitude compared to simulations using nonlinear models [Eqs. (14)–(18)].

https://doi.org/10.1017/S0263034601193134 Published online by Cambridge University Press

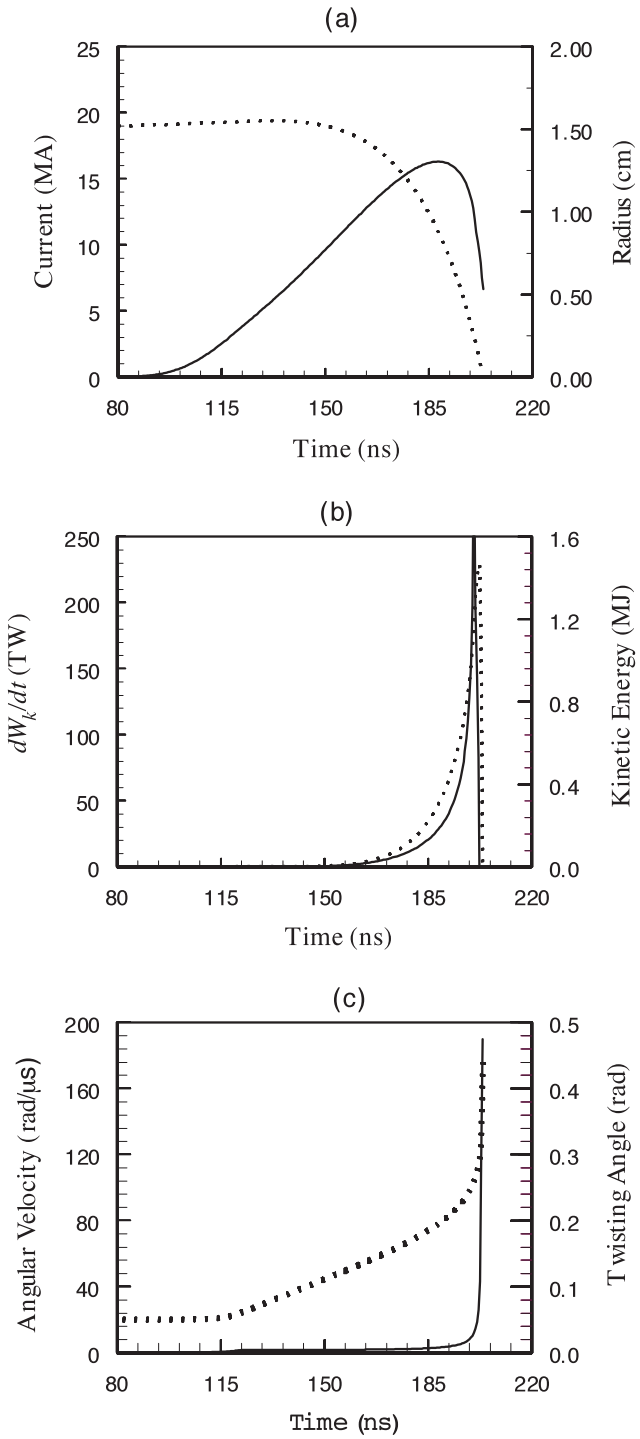

Fig. 3. (a) The current (solid line) and maximum load radius (dotted line) for an S-pinch load with $\Delta = 0.2$, $\beta = 0.05$; (b) time histories of the radial kinetic energy W_k (dotted line) and the mechanical power W_k/dt (solid line); (c) the rotation velocity (solid line) and the twisting angle (dotted line).

The dynamics of a plasma shell with a perturbed outer surface is shown at four subsequent times prior to stagnation for a straight, cylindrical wire array in Figure 5, and for wires initially twisted along the curved surface in Figure 6.

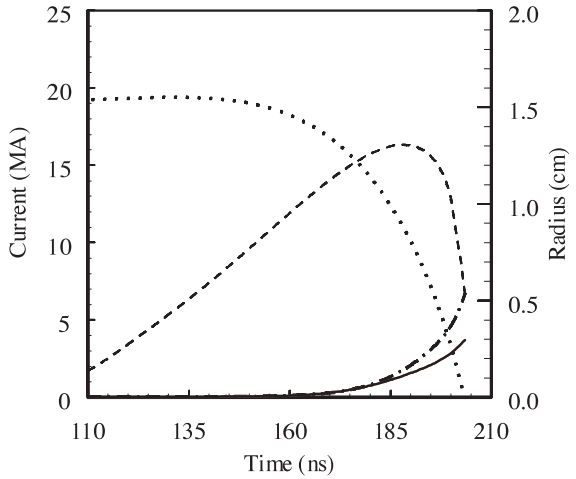

Fig. 4. Dynamics of a wire array load and the R-T instabilities: The current through the load (dashed line), the load radius (dotted line), the bubble amplitude (solid line), the spike amplitude (dotted-dashed line) of the R-T instability for an initial amplitude 0.02 mm and a wave number $k = 2.2\ \mathrm{mm}^{-1}$.

The calculations demonstrated that the shell is less disrupted by the R-T perturbations in the case of initially twisted wires, as the instabilities are localized to the central cross section of the load.

By varying the initial twist angle and the surface curvature, we found that an optimum design would have the wires twisted initially with an angle in the range from 0.05 to 0.08 and an initial load curvature in the range from 1 to 2 mm. For these loads, the greatest possible values of the kinetic energy and X-ray power are calculated. The R-T instabilities break through the plasma shell only when the internal radius of the shell is close to zero, that is, prior to stagnation.

Calculations show that an initially twisted load design provides a more efficient energy transfer from the pulsed-power generator to the load compared with a straight, cylindrical wire array. Rough estimates predict a minimum 20% increase in the kinetic energy of a load prior to stagnation. According to estimates provided by Mosher *et al.* (1998), *K*-shell radiation yield, *Y*, scales with the kinetic energy, E_k, as $Y \sim E_k^2$. One can extrapolate this dependence and expect a significant increase in radiation yield, even if only 50% of the load kinetic energy can be attributed to radiation as suggested by Spielman *et al.* (1998).

The simulations also revealed that the initially twisted load accelerates faster during the implosion. Comparing Figure 5d and Figure 6d, one can see that the inner surface of the plasma shell reaches the axis of symmetry a few nanoseconds earlier in the case of initially twisted wires. In this case, the azimuthal velocity increases significantly during implosion compared to the classical *z* pinch, which promotes faster growth of the R-T instabilities. However, our simulations of the nonlinear stage of the R-T growth show that this increase in the R-T instability amplitude is not severe and ceases when the inner surface of the plasma shell reaches the axis of symmetry. This occurs earlier in case of

https://doi.org/10.1017/S0263034601193134 Published online by Cambridge University Press

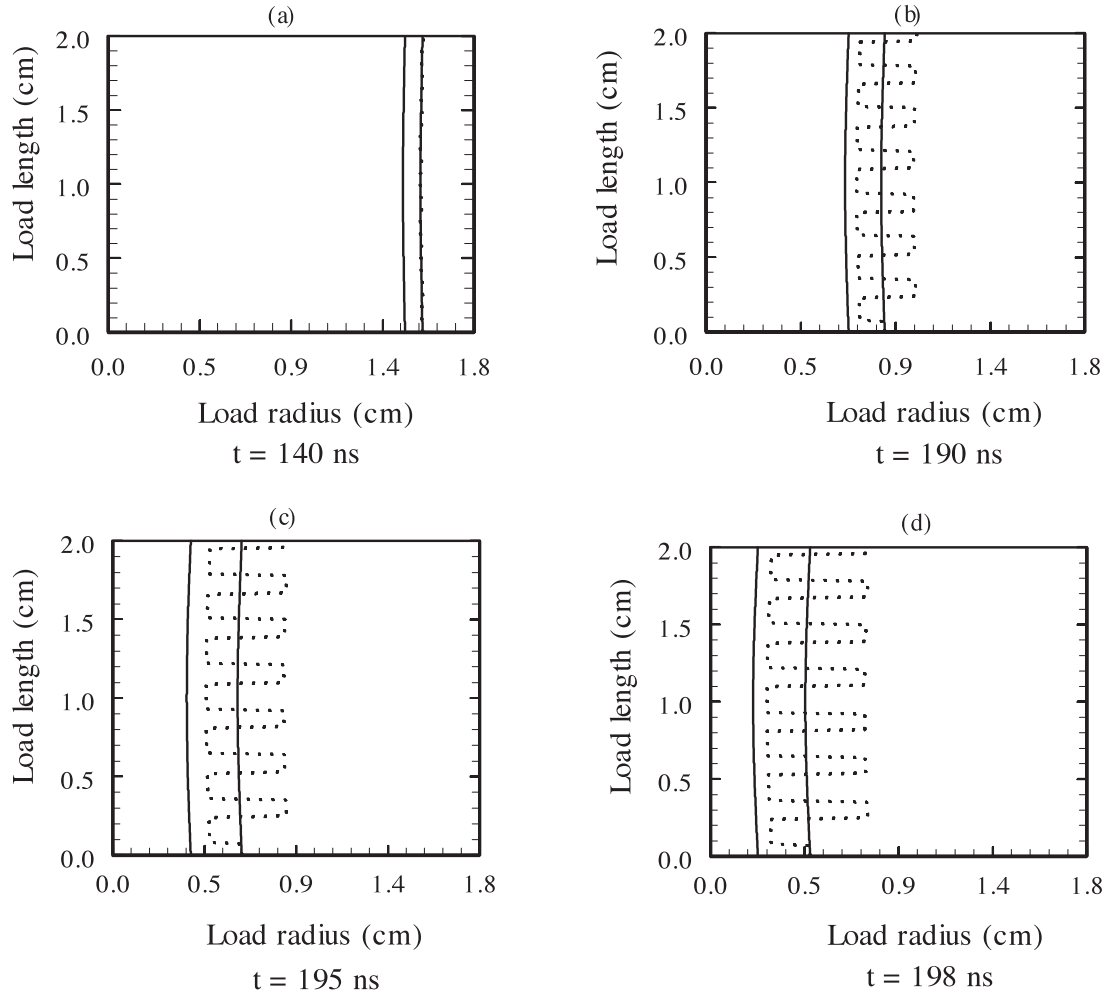

Fig. 5. The calculation shows the development of the R-T perturbation for $k = 2.2$ mm^{-1} on the flat surface of the imploding plasma shell at four different times prior to the stagnation: the inner and outer surface of a plasma shell (solid line) and the R-T perturbation on the outer surface (dotted line).

an initially twisted load. In addition, the increase of the azimuthal velocity is expected to intensify the process of turbulent mixing and, therefore, to increase the efficiency of the conversion of kinetic energy into radiation.

Various configurations of twisted (S-pinch) loads in the return current can with inclined slots (Fig. 7) were simulated numerically. Time histories of the current through the load and the wire array radius near the electrodes are shown along with the amplitudes of a spike and a bubble in Figure 8a, the radial load velocity, growth rates for spike and bubble in Figure 8b, and energy partition components in Figure 8c. The load kinetic energy, the energy of azimuthal magnetic field, and the energy of axial magnetic field are denoted by E_k, E_{mfi}, and E_{mz}, respectively. The energy of the radial magnetic field is negligible. The dynamics of a plasma shell with the R-T instabilities for simulations corresponding to Figure 8 are shown in Figure 9.

4. DISCUSSION

It was shown that an optimum design would have the wires twisted initially with an angle in the range from 0.05 to 0.08 and with an initial load curvature in the range from 1 to 2 mm. For these loads, the greatest possible values of the kinetic energy and X-ray power are calculated, while the R-T instabilities break a plasma shell only when the internal radius of the shell is close to zero, that is prior to stagnation. By varying the initial twist angle, surface curvature, inclination angle for slots in the current return can, we observed the simulated effect of using current return can with inclined slots for both *z* pinches and S pinches to generate the magnetic field for stable implosions. Obviously, the increase of the inclination angle results in the increase of the initial inductance of the load and the energy of the compressed axial magnetic field constituting a significant portion of the

https://doi.org/10.1017/S0263034601193134 Published online by Cambridge University Press

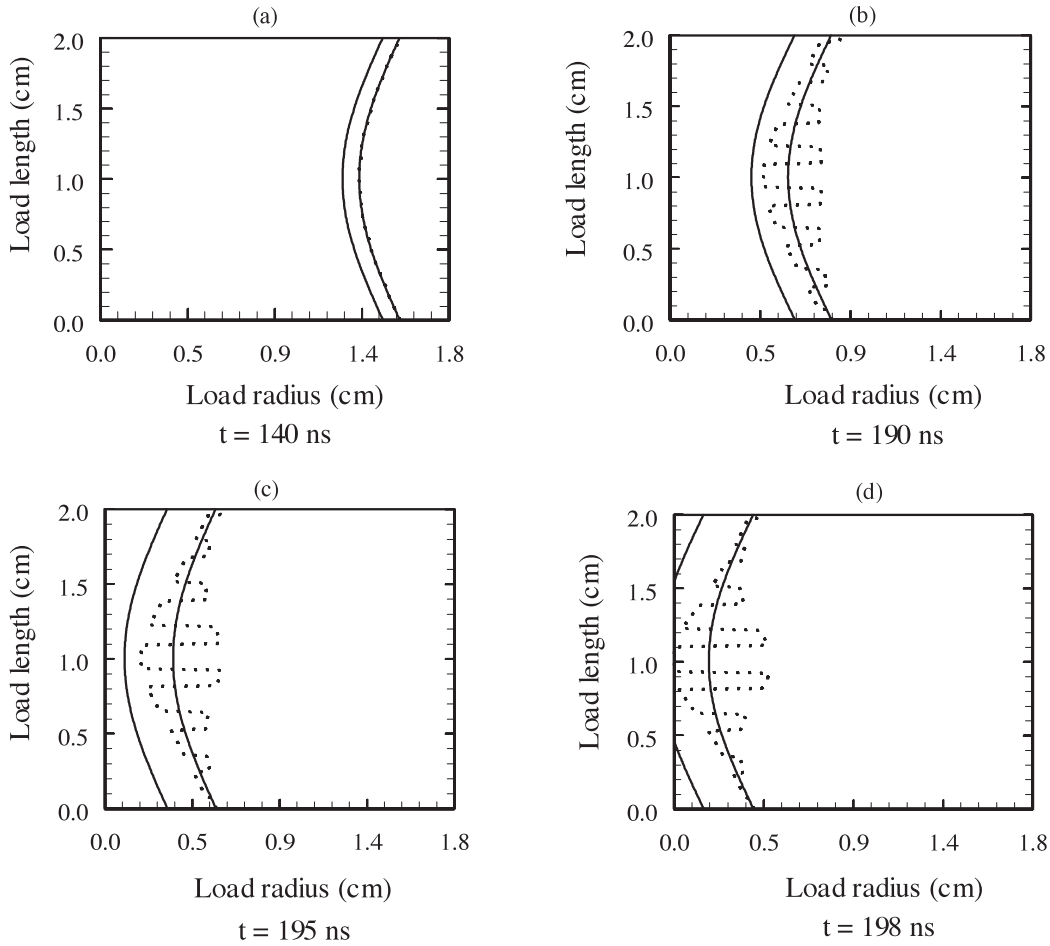

Fig. 6. The calculation shows the development of the R-T perturbation on the curved surface of the twisted plasma shell at four different times prior to the stagnation: the inner and outer surface of a plasma shell (solid line) and the R-T perturbation on the outer surface (dotted line). The initial twist angle is 0.08 and the initial surface curvature is 2 mm.

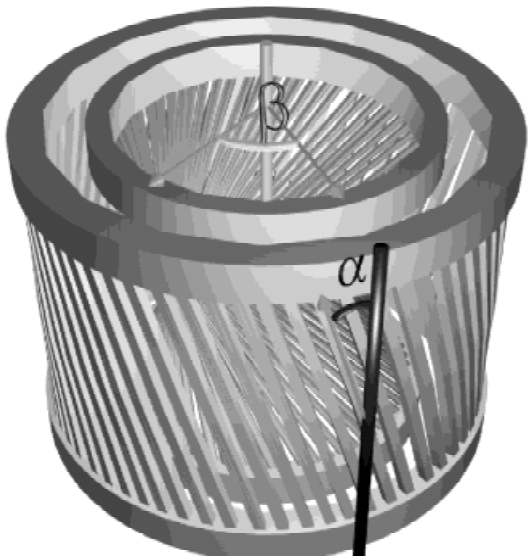

Fig. 7. Schematic design of a twisted wire array load with a return current can with inclined slots.

energy delivered to a load from the pulsed power generator. This results in the decrease in the kinetic energy of the load (see Fig. 10). However, azimuthal velocity increases, and this, in our opinion, should strengthen the process of turbulent mixing, and hence the dissipation of the axial magnetic field. Unfortunately, 0-D calculations cannot provide qualitative estimates for this effect.

It is recommended to use a higher number of inclined slots instead of a few slots, because current return can is located only 5 mm away from the wire array and very few slots could cause additional azimuthal nonuniformity of the imploded plasma pinch. In the experiments (Sorokin & Chaikovsky, 1993), the return current solenoid was formed by 24 rods placed at a 45° angle to the cylindrical surface generatrix.

The use of a current return can with inclined slots causes faster acceleration of the twisted load due to the additional Lorentz force. Figure 11 shows the time when the inner surface of the shell hits the axis as a function of the slot inclination angle.

https://doi.org/10.1017/S0263034601193134 Published online by Cambridge University Press

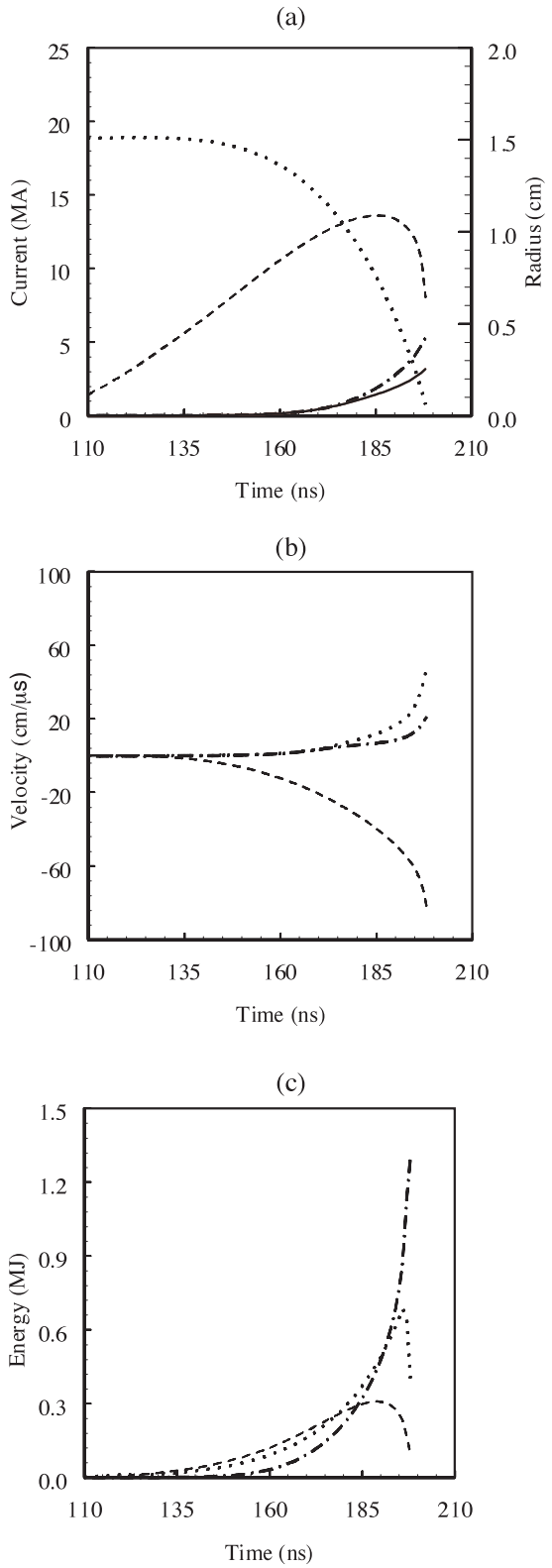

Fig. 8. Dynamics of a wire array load and the R-T instabilities: (a) The current through the load (dashed line), the load radius (dotted line), the bubble amplitude (solid line), and the spike amplitude (dotted-dashed line) of the R-T instability; (b) the radial load velocity (dashed line) and growth rates for spike (dotted line) and bubble (dotted-dashed line); (c) load kinetic energy (dotted-dashed line), the energy of azimuthal magnetic field (dashed line), and the energy of axial magnetic field (dotted line).

Calculations show that the greater the inclination angle of the return current slots, the greater the B_z value is. At the same time, greater B_z results in less radial kinetic energy of the load. However, Spielman *et al.* (1998) suggested that only 50% of the radiation energy can be directly attributed to the conversion of kinetic energy and the remaining energy is associated with the compression of the stagnated plasma by the magnetic pressure force. We believe that there exist optimum conditions in which the current return can with inclined slots promotes stabilization of the plasma shell formed by wires in the initial stage of implosion and at the same time a sufficient amount of kinetic energy is delivered to the load, which is further converted into the radiation. The exact optimal conditions could not be found with 0-D calculations though we could offer a range for variables for experiments.

An optimum load design is suggested to have the wires twisted initially with an angle in the range from 0.05 to 0.08 and with an initial load curvature in the range from 1 to 2 mm. Our analysis of calculations suggests that inclination angle $\pi/50$ and about 40–50 inclined slots could be recommended for experiments.

5. CONCLUSION

In conclusion, we have found that a multi-wire screw pinch, a variant of a *z*-pinch load is a possible way to achieve higher X-ray radiation. The 0-D implosion simulations show that a moderate initial twist of the wires along the curved surface results in the accelerated rotation of the wire arrays and the plasma shell during the implosion. This rotation is expected to have a doubly positive effect on the load performance. First, it will stabilize the growth of large-scale perturbations of the R-T instability and will improve the uniformity of the load, and, second, it will promote turbulent flows in a *z*-pinch plasma prior to the stagnation stage. Therefore, an S-pinch load design is expected to provide the higher X-ray radiation power.

The effect of initially twisting a multiwire, *z*-pinch plasma load on the large wavelength R-T instability growth and X-ray radiation was studied. The self-consistent simulation of the implosion of a plasma shell with wire cores and the development of the R-T perturbations was carried out for both classical multiwire *z*-pinch loads and initially twisted wire arrays. The results of these calculations demonstrated that the shell is less disrupted by the R-T perturbations in the case of initially twisted wire arrays, as the instabilities are localized to the central cross section of the load. Because the inductance of a twisted wire array increases more quickly, the load acceleration is higher compared to the acceleration for a classical *z* pinch. Higher acceleration causes the higher R-T growth; however, this increase is not significant and, in the range of parameters considered for the load, is found not to disrupt the imploding plasma shell prior to stagnation. The kinetic energy of the twisted load prior to stagnation increases more than 20% compared to a straight, cylindrical

https://doi.org/10.1017/S0263034601193134 Published online by Cambridge University Press

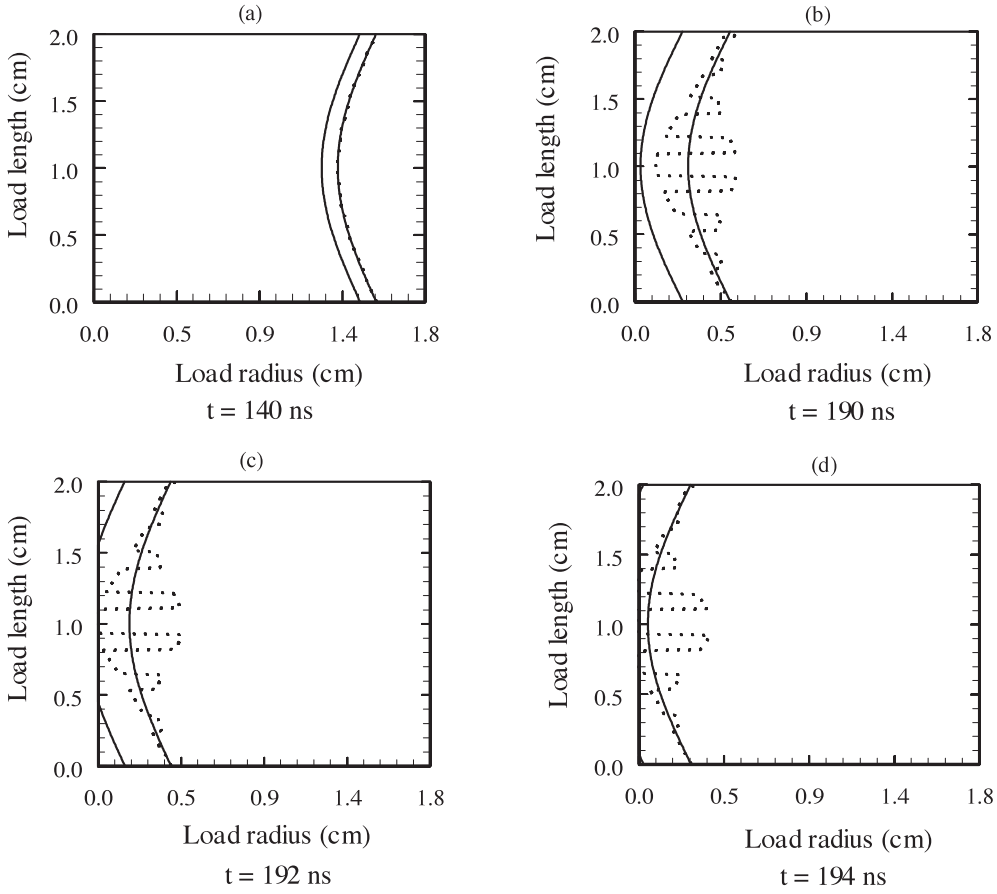

Fig. 9. The calculation shows the development of the R-T perturbation on the curved surface of the twisted plasma shell inside of the return current can with 5° inclined slots at four different times prior to the stagnation: the inner and outer surface of plasma shell (solid line) and the R-T perturbation on the outer surface (dotted line).

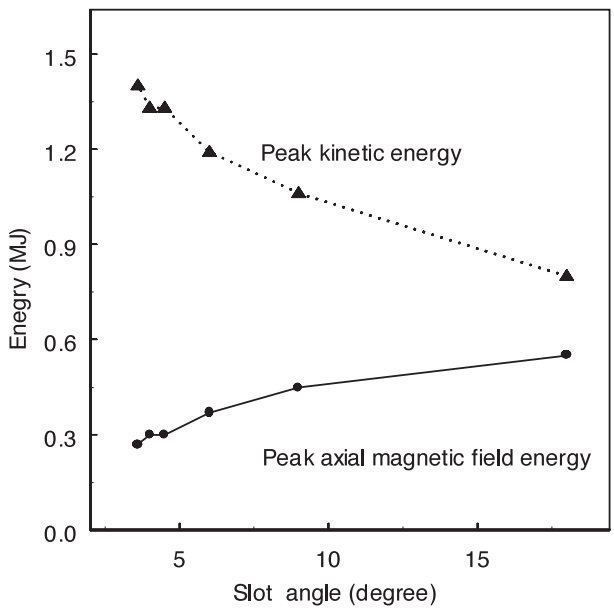

Fig. 10. The dependence of the peak energy components on the slot inclination angle.

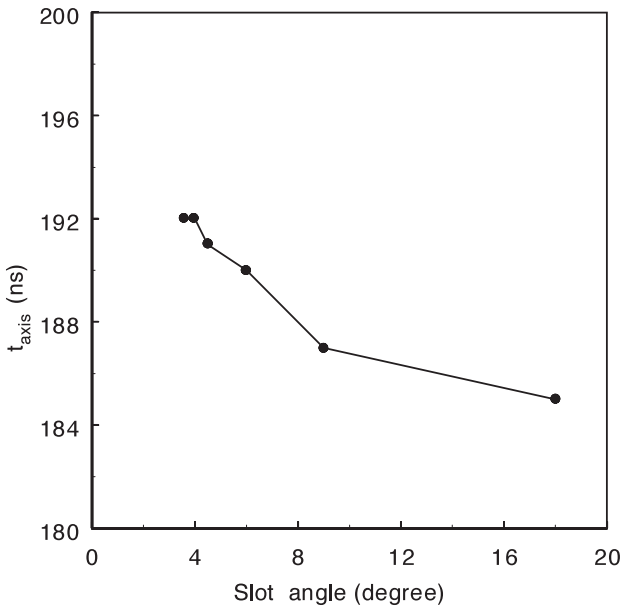

Fig. 11. The dependence of an instance in time when the inner surface of the shell hits the axis on the slot inclination angle.

https://doi.org/10.1017/S0263034601193134 Published online by Cambridge University Press

wire array, giving the potential for a significantly higher X-ray yield. The model may also be useful for analysis of long-pulse *z*-pinch implosions.

Future experiments are required for a more quantitative study of the effect of various physical factors on the generation of X rays. Analytical and computational analyses of the laminar-turbulent transition process (Volkov *et al.*, 1999*a*) and simulations with the hydrodynamic model for plasma with strong macroscopic turbulence (Landau & Lifschits, 1973) would provide an insight into fundamental questions on mechanisms of thermodynamic equilibrium, the role of X-ray radiation, and the conversion of kinetic energy into X-ray radiation at the stagnation stage.

ACKNOWLEDGMENTS

This work was supported by Sandia National Laboratories and partially by the Russian Foundation for Basic Research *via* Grant No. 97-02-16177.

REFERENCES

Baker, L. & Freeman, J.R. (1980). *J. Appl. Phys.* **52**, 655.
Branitskii, A.V. *et al.* (1999). *Sov. Fiz. Plasmi* **25**, 1060.
Chandrasekhar S. (1961). *Hydrodynamic and Hydromagnetic Stability*. Oxford: Clarendon Press.
Davis, J. *et al.* (1997). *Appl. Phys. Lett.* **70**, 170.
Deeney, C. *et al.* (1998). *Phys. Plasmas* **5**, 2431.
Deeney, C. *et al.* (1999). *Phys. Plasmas* **6**, 3576.
Douglas, M.R. *et al.* (1997). *Phys. Rev. Lett.* **78**, 4577.
Fermi, E. (1972). *Scientific Works*. Moscow: Nauka.
Gasque, A.M. *et al.* (1998). *Sov. Fiz. Plasmi*, **24**, 726.
Gersten, M. *et al.* (1986). *Bull. Am. Phys. Soc.* **29**, 2050.
Golub, T.A. *et al.* (1997*a*). *Bull. Am. Phys. Soc.* **42**, 2051.
Golub, T.A. *et al.* (1997*b*). In *Proc. 11th Int. Pulsed Power Conf.*, p. 832. New York: IEEE, Inc.
Golub, T.A. *et al.* (1999*a*). In *Proc. of the 12th Int. Pulsed Power Conf.* (*IEEE Trans. Plasma Sci.* (2000), **28**, 1422).
Golub, T.A. *et al.* (1999*b*). *Bull. Am. Phys. Soc.* **44**, 102.
Gus'kov, S.Yu. *et al.* (1998). *Pis'ma v JET* **67**, 531.
Iskoldsky, A.M. *et al.* (1996). *Physica D* **91**, 182.
Landau, L.D. & Lifschits, E.M. (1973). *Mechanics*. Moscow: Nauka.
Liberman, M.A. *et al.* (1999). *Physics of High-Density Z-Pinch Plasmas*. New York: Springer-Verlag.
Loskutov, V.V. & Luchinsky, A.V. (1995). *Izvestiya VUZ'ov: "Fizika"* **12**, 16.
Marder, B. & Desjarlais, M. (1998). In *Abstracts of IEEE International Conference on Plasma Science*, Raleigh, NC. p. 268. New York: IEEE, Inc.
Mosher, D. *et al.* (1998). *IEEE Trans. on Plasma Sci.* **26**, 1052.
Neyman, L.R. & Demirchan, K.S. (1981). *Theoretical Fundamentals of Electrical Engineering*, vol. 2, p. 323, Leningrad: Energoizdat.
Oreshkin, V. (1995). *Izvestiya VUZ'ov: Fizika* **6**, 12.
Pikuz, S.A. *et al.* (1999). *Phys. Rev. Lett.* **81**, 4313.
Rudakov L.I. & Sudan R.N. (1997). *Phys. Reports* **283**, 253.
Shelkovenko, T.A. *et al.* (1998). In *Abstracts of IEEE Int. Conf. on Plasma Sci.*, Raleigh, NC, p. 121. New York: IEEE, Inc.
Shneerson, G.A. (1992). *Fields and Transient Phenomena into Extra-High Current Apparatus*. Moscow: Energoatomizdat.
Spielman, R.B. *et al.* (1998). *Phys. Plasmas* **5**, 2105.
Sorokin S.A. & Chaikovsky S.A. (1993). *Sov. Fiz. Plasmi* **19**, 856.
Sorokin S.A. *et al.* (1991). *Sov. Fiz. Plasmi* **17**, 1453.
Thornhill J.W. *et al.* (1994). *Phys. Plasmas* **1**, 321.
Volkov, N.B. (1999). *Plasma Phys. and Controlled Fusion* **41**, 1025.
Volkov, N.B. & Zubarev, N.M. (1995). *JETP* **80**, 1037.
Volkov, N.B. *et al.* (1976). *Isvestiya Akademii Nauk: "Energetika i transport"* **6**, 146.
Volkov, N.B. *et al.* (1999*a*). *Bull. Am. Phys. Soc.* **42**, 2051.
Volkov, N.B. *et al.* (1999*b*). *Appl. Phys. Lett.* **74**, 3624.
Wessel, F.J. *et al.* (1986*a*). *Bull. Am. Phys. Soc.* **29**, 1474.
Wessel, F.J. *et al.* (1986*b*). *Appl. Phys. Lett.* **48**, 28.